Polycationic Nanoparticles for siRNA Delivery: Comparing ARGET ATRP and UV-Initiated Formulations

Diane C. Forbes[†] and Nicholas A. Peppas[†,‡,§,*]

[†]Department of Chemical Engineering, [‡]Department of Biomedical Engineering, and [§]College of Pharmacy, The University of Texas at Austin, Austin, Texas 78712, United States

ABSTRACT In this work, we develop and evaluate polycationic nanoparticles for the delivery of small interfering RNA (siRNA). Delivery remains a major challenge for translating siRNA to the clinic, and overcoming the delivery challenge requires effective siRNA delivery vehicles that meet the demands of the specific delivery strategy. Cross-linked polycationic nanoparticle formulations were synthesized using ARGET ATRP or UV-initiated polymerization. The one-step, one-pot, surfactant-stabilized monomer-in-water synthesis technique may provide a simpler and faster alternative to complicated, multistep techniques and an alternative to methods that rely on toxic organic solvents. The polymer nanoparticles were synthesized using the cationic monomer 2-(diethylamino)ethyl methacrylate, the hydrophobic monomer *tert*-butyl methacrylate to tune pH responsiveness, the hydrophilic monomer poly(ethylene glycol) methyl ether methacrylate to improve biocompatibility, and cross-linking agent tetraethylene glycol dimethacrylate to enhance colloidal stability. Four formulations were evaluated for their suitability as siRNA delivery vehicles *in vitro* with the human embryonic kidney cell line HEK293T or the murine macrophage cell line RAW264.7. The polycationic nanoparticles demonstrated efficient and rapid loading of the anionic siRNA following complexation. Confocal microscopy as well as flow cytometry analysis of cells treated with polycationic nanoparticles loaded with fluorescently labeled siRNA demonstrated that the polycationic nanoparticles promoted cellular uptake of fluorescently labeled siRNA. Knockdown experiments using polycationic nanoparticles to deliver siRNA demonstrated evidence of knockdown, thus demonstrating potential as an alternative route to creating polycationic nanoparticles.

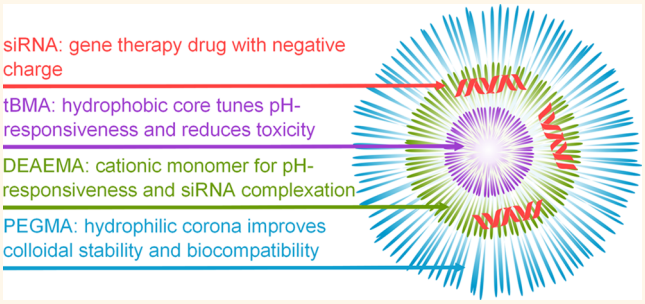

KEYWORDS: ARGET ATRP · cationic polymer · drug delivery · siRNA · UV-initiated

While drug delivery systems for small interfering RNA (siRNA) have been extensively studied, the challenges associated with safe and effective delivery continue to prevent widespread translation of the new technology from the bench to the clinic.[1−4] RNA interference (RNAi) induced by small noncoding RNAs is a post-transcriptional mechanism to down-regulate gene expression by potently and specifically degrading mRNA, thus preventing translation of the mRNA to protein.[5] siRNA has been likened to a "magic bullet"[6] due to this potency and specificity, but as with *Der Freischütz*, off-target effects (which can occur *via* an miRNA-like mechanism by degradation of mRNA sequences with partial complementary) create additional challenges for researchers.[7,8]

Unprotected oligonucleotides such as naked, unmodified siRNA have a very short half-life *in vivo* (seconds to minutes)[9] as a result of loss of functionality from degradation (by endogenous nucleases)[10] and rapid kidney filtration from circulation (due to their small size).[11] Following cellular internalization, the siRNA must also escape the endosome because siRNA must be inside the cytosol (rather than sequestered in a subcellular compartment) to have a therapeutic effect.[12] For these reasons, enhanced delivery strategies such as novel nanoparticle structures are necessary to prevent degradation or clearance, to enhance uptake, and to promote endosomal escape.

Some cell types, such as primary cells,[13] cells of the central nervous system,[14] and macrophage-type cell lines like the murine

* Address correspondence to peppas@che.utexas.edu.

Received for review January 8, 2014 and accepted February 18, 2014.

Published online February 18, 2014
10.1021/nn500101c

TABLE 1. Transfection of HEK293 Cells with siRNA: Examples from the Literature[a]

type of carrier	concentration and type of siRNA	method of evaluating knockdown	ref
imidazole-4-acetic acid (IAA)-conjugated chitosan	50 nM GAP480 silencer siRNA	KDalert assay kit	25
siPORT amine	20 nM GAPDH siRNA	KDalert assay kit	26
micelle nanoparticles ($mPEG_{45}$-*b*-PCL_{100}-*b*-PCL)	100 nM EGFP siRNA	flow cytometry to measure GFP expression	27
micelle nanoparticles ($mPEG_{45}$-*b*-PCL_{100}-*b*-PCL)	GL3 luciferase siRNA	luminescence	27
Lipofectamine2000	10 nM of various siRNAs	luminescence, ELISA, RT-PCR, Western blotting	28
layered double hydroxide nanoparticles	250 nM siRNA DCC gene	Western blotting	29

[a] DCC, deleted in colorectal cancer; (E)GFP, (enhanced) green fluorescent protein; ELISA, enzyme-linked immunosorbent assay; mPEG, methoxypoly(ethylene glycol); PCL, poly(ε-caprolactone); RT-PCR, reverse transcriptase polymerase chain reaction.

TABLE 2. Transfection of RAW264.7 Cells with siRNA: Examples from the Literature[a]

type of carrier	concentration and type of siRNA	method of evaluating knockdown	ref
PEI-PLGA microparticles	25—30 nM IL-10 siRNA	RT-PCR	26
Dharmafect, Lipofectamine2000, HiPerfect, and other commercial transfection agents	20—100 nM EGFP siRNA	green fluorescence quantified using an automated fluorescence microscope	15
rabies virus glycoprotein conjugated nona-D-arginine residues (RVG-9dR)	200 nM TNF-α siRNA	TNF-α ELISA, RT-PCR	30
thioketal nanoparticles	1500—2000 nM TNF-α siRNA	TNF-α ELISA	31
PEI nanoparticles	1 nM TNF-α siRNA	TNF-α ELISA	32
mannose-modified trimethyl chitosan—cysteine (MTC) conjugate nanoparticles	1—300 nM TNF-α siRNA	TNF-α ELISA, RT-PCR	33
amphiphilic cationic cyclodextrin	100 nM TNF-α siRNA	TNF-α and IL-6 ELISA, RT-PCR	34
cationic shell cross-linked knedel-like nanoparticles (cSCKs)	100 nM AllStars Death siRNA	MTS to measure relative cell viability	35

[a] Macrophage-type cells like RAW264.7 are considered to be difficult to transfect.[15] (E)GFP, (enhanced) green fluorescent protein; ELISA, enzyme-linked immunosorbent assay; PEI, polyethylenimine; PLGA, poly(lactide-*co*-glycolide); RT-PCR, reverse transcriptase polymerase chain reaction; TNF-α, tumor necrosis factor α.

macrophage cell line RAW264.7,[15] are considered difficult to transfect, while other cell types such as the human embryonic kidney cell line HEK293T are widely used for siRNA screen experiments. (For examples of siRNA knockdown in the literature using RAW264.7 or HEK293T cell lines, see Table 1 and Table 2, respectively.) Note that since a brief search for articles referencing siRNA in a major literature search service reveals 100000s of articles, and these articles likely represent 1000s—10000s of distinct delivery strategies to 10s—100s of cell types, the types listed in the tables represent only a small fraction of the siRNA delivery experiments reported in the literature. Within this legion of delivery strategies, the majority of siRNA delivery experiments rely upon carrier-mediated delivery, such as complexation of the siRNA to cationic lipids. Early (and largely disappointing) siRNA-based therapeutic clinical trials relied upon the delivery of naked siRNA, but later clinical trials for siRNA-based therapeutics have relied upon sophisticated delivery vehicles for carrier-mediated delivery.[5]

Effective nanoparticle vehicles for drug delivery must demonstrate siRNA binding, low cytotoxicity, effective cellular uptake, and, most importantly, evidence of siRNA-induced knockdown. While reports of advanced or complex chemistry techniques indicate that these new methods may have promise as effective nanoparticle carriers, there are few examples in the literature that provide a direct comparison of ARGET ATRP (activators regenerated by electron transfer atom transfer radical polymerization) and UV-initiated polycationic nanoparticles. Of these few examples that provide a direct comparison of ARGET ATRP and UV-initiated polymerization, none (to the best of the authors' knowledge) directly compare siRNA delivery for the two different methods. This work evaluates polycationic nanoparticles synthesized by either ARGET ATRP or UV-initiated polymerization and provides the first report of their suitability as siRNA delivery vehicles to HEK293T and RAW264.7 cells.

RESULTS AND DISCUSSION

Synthesis of Polycationic Nanoparticles. Polycationic nanoparticles were synthesized using a previously reported ARGET ATRP technique[16,17] or a UV-initiated polymerization technique previously developed by Fisher *et al.*[18] The techniques represent single-step, one-pot, surfactant-stabilized monomer-in-water synthesis methods that may provide a simpler and faster alternative to complicated multistep techniques and an alternative to methods that rely on toxic organic solvents. The polycationic nanoparticles are composed of the cationic monomer 2-(diethylamino)ethyl methacrylate (DEAEMA), the hydrophobic monomer *tert*-butyl methacrylate (tBMA) to tune pH responsiveness, the hydrophilic monomer poly(ethylene glycol) methyl ether methacrylate (PEGMA) to improve biocompatibility, and cross-linking agent tetraethylene glycol dimethacrylate (TEGDMA) to enhance colloidal stability.

Two different molar feed compositions were examined, differing in the mole ratio of tBMA to DEAEMA in the feed (30 or 45 mol tBMA per 100 mol DEAEMA in the feed). The tBMA composition of the feed was varied as previous work by Fisher *et al.* had demonstrated that tBMA played an important role in modulating the properties of polycationic nanoparticles.[19]

The physical characterization of the four formulations of P(DEAEMA-*co*-tBMA-*co*-PEGMA-*co*-TEGDMA) polycationic nanoparticles has been presented in the literature.[16,17] Briefly, dynamic light scattering demonstrates a positive surface charge (zeta-potential of ~40 mV in water) with a z-average diameter of ~75 to ~150 nm (in 1× PBS pH 7.4), with increased size associated with the ARGET ATRP formulations compared to the UV-initiated formulations and also for the 30 mol tBMA formulations compared to the 45 mol tBMA formulations.[16] In addition, the ARGET ATRP formulations demonstrated sharper pH-responsive[16] and thermal[17] transitions than the corresponding UV-initiated formulations.

Binding of siRNA. The loading efficiency of the polycationic nanoparticles is related to the siRNA binding, and the binding of siRNA to polycationic nanoparticles was evaluated using the RiboGreen assay. The siRNA demonstrates efficient loading even after 10 min, with 85−91% loading efficiency for all polycationic nanoparticle formulations (Figure 1). After 70 min incubation, the loading efficiency demonstrates a nominal increase to 96−98% efficiency for all polycationic nanoparticle formulations, and this efficiency persists after 160 min. Based on the negligible increase in siRNA from 10 to 70 min, the siRNA/nanoparticle complexes were used shortly after preparation (approximately 10 min after adding the siRNA) rather than after a longer incubation. At all time points, there is no significant difference in siRNA binding among the four formulations.

The siRNA demonstrates very efficient binding (~98% for all formulations) in 0.2× PBS pH 5.5, likely due to positive charge induced by low pH combined with low ionic strength (Figure 2). Across all formulations, the siRNA binding follows the following decreasing trend: 0.2× PBS pH 5.5 > 1× PBS pH 5.5 > 1× PBS pH 7.4 > Opti-MEM. For the 1× PBS pH 7.4 and the Opti-MEM, the 30UV and 30ARGET formulations demonstrate slightly higher binding efficiencies than the corresponding 45UV and 45ARGET formulations. The 45ARGET formulation demonstrates the lowest binding efficiency in Opti-MEM of the four formulations, with 55% of the siRNA bound to the polymer (compared to 74% for 30UV, 70% for 45UV, and 63% for 30ARGET). The reduced binding efficiency for 45ARGET compared to that of the other formulations may be a factor in determining knockdown efficiency; however, it is one factor among many.

Nanoparticle Cytotoxicity. The biocompatibility of the polycationic nanoparticles with HEK293T cells and

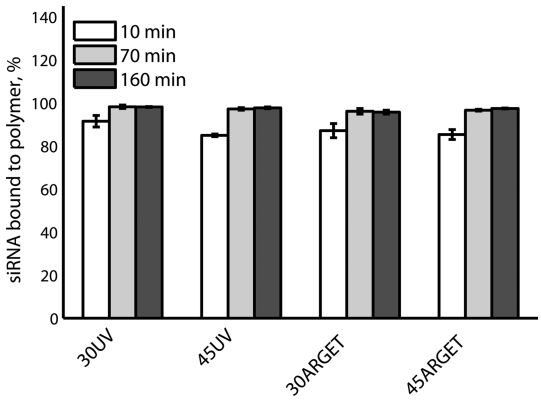

Figure 1. Binding of siRNA to polycationic nanoparticles. Nanoparticles were loaded with AllStars negative control siRNA in 1× PBS pH 5.5, with 0.125 mg/mL nanoparticles and 500 nM siRNA. Binding of siRNA evaluated at 10, 70, and 160 min using RiboGreen. Data are expressed as the mean plus or minus the standard deviation (*n* = 3).

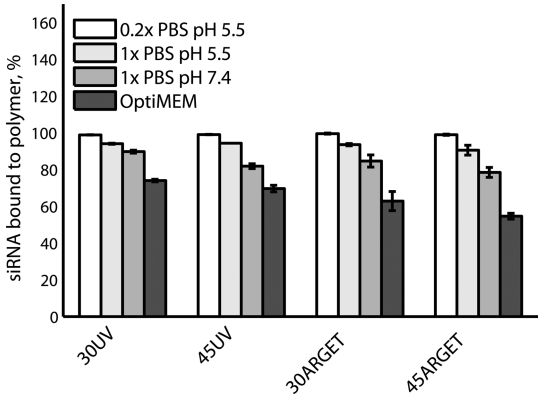

Figure 2. Binding of siRNA to polycationic nanoparticles in PBS buffers and Opti-MEM. Following loading of 0.125 mg/mL nanoparticles with 500 nM siRNA, complexes were diluted 5× in 0.2× PBS pH 5.5, 1× PBS pH 5.5, 1× PBS pH 7.4, and Opti-MEM prior to evaluating siRNA binding using RiboGreen. Data are expressed as the mean plus or minus the standard deviation (*n* = 3).

RAW264.7 cells was evaluated using an MTS assay following 48 h incubation with the nanoparticles (see Figure 3). Both cell lines demonstrate high relative viability at low concentrations (greater than 80% viability at 0.025 mg/mL and lower concentrations). In HEK293T cells, formulations 45UV and 45ARGET show increased biocompatibility compared to the 30UV and 30ARGET formulations; for example, at 0.05 mg/mL, the 45UV and 45ARGET formulations demonstrate 60 and 78% viability, respectively, while the 30UV and 30ARGET formulations demonstrate 18 and 21% viability, respectively.

In the RAW264.7 cells, biocompatibility is less dependent on formulation. The biocompatibility of the polycationic nanoparticle formulations with the RAW264.7 cells is indistinguishable at the upper two (0.2 and 0.1 mg/mL) and lower two (0.00313 and 0.00156 mg/mL) concentrations. Both 30ARGET and 45ARGET show a slightly increased viability compared

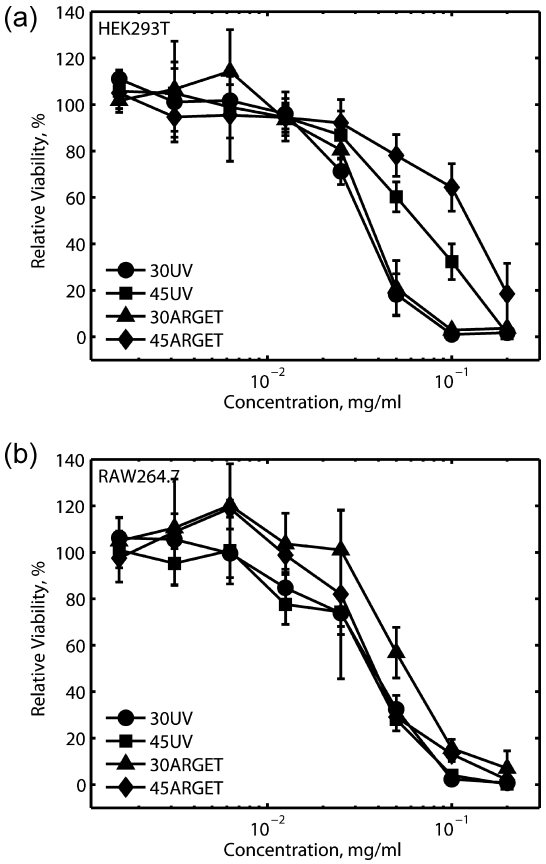

Figure 3. Biocompatibility of polycationic nanoparticle formulations with (a) HEK293T cells or (b) RAW264.7 cells at various concentrations (0.02−0.00156 mg/mL) evaluated using an MTS assay following 48 h incubation. Data are expressed as the mean plus or minus the standard deviation (n = 6).

to 30UV and 45UV at 0.05 and 0.025 mg/mL in RAW264.7 cells. At 0.0625 mg/mL, the 30ARGET shows increased viability compared to the other three formulations (100% *versus* 74−82% viability). All formulations demonstrated low viability in both cell types at the highest concentration tested (0.2 mg/mL).

Flow Cytometry To Quantify Uptake of Fluorescently Labeled siRNA. Flow cytometry was used to evaluate the internalization of fluorescently labeled siRNA. The percent of cells associated with fluorescently labeled siRNA and the normalized fluorescent intensity for each formulation are shown in Figure 4 and Figure 5, respectively (see Supporting Information for representative histograms). All polycationic nanoparticles demonstrated efficient uptake with slight differences among formulations in the percentage of cells with fluorescently labeled siRNA. However, the difference between cell types is more significant. When the siRNA is delivered with polycationic nanoparticles, a greater percentage of RAW264.7 cells than HEK293T cells shows fluorescence of DY647 siRNA. For the polycationic nanoparticle formulations with HEK293T cells, 50.8 to 60.8% of cells are associated with fluorescently labeled siRNA; likewise, the comparable values for the RAW264.7 cells

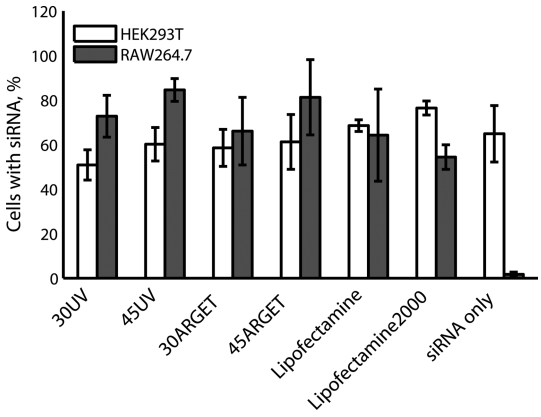

Figure 4. HEK293T or RAW264.7 cells associated with fluorescently labeled DY647 siRNA. Cells were incubated for 2 h with 0.05 mg/mL polycationic nanoparticles or appropriate controls with 200 nM fluorescently labeled DY647 siRNA. Following incubation, cells were rinsed and suspended for flow cytometry analysis with a BD Fortessa flow cytometer. Data are expressed as the mean plus or minus the standard deviation of three independent experiments.

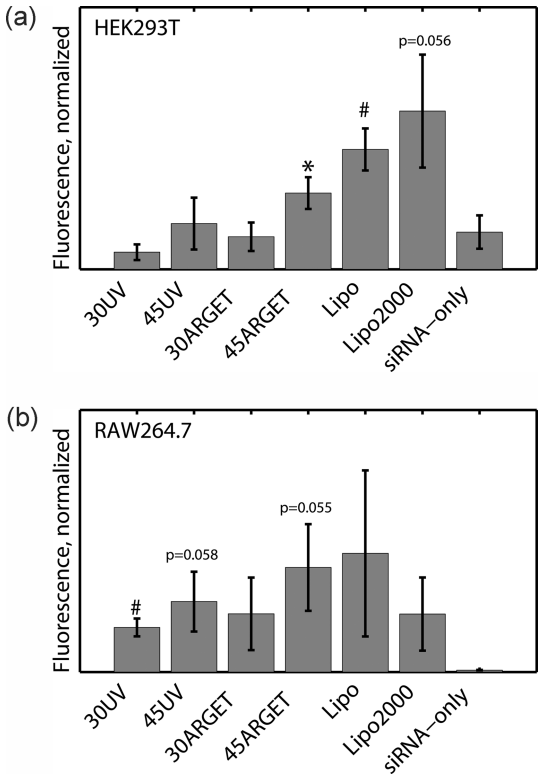

Figure 5. (a) HEK293T or (b) RAW264.7 cells associated with fluorescently labeled DY647 siRNA. Cells were incubated for 2 h with 0.05 mg/mL polycationic nanoparticles or appropriate controls with 200 nM fluorescently labeled DY647 siRNA. Following incubation, cells were rinsed and suspended for flow cytometry analysis with a BD Fortessa flow cytometer. Data are expressed as the mean plus or minus the standard deviation of three independent experiments. The data are normalized by dividing by the fluorescence intensity of the blank PBS-only control. Asterisks (*) and pound signs (#) represent $p < 0.05$ and $p < 0.015$, respectively, as determined using Student's t test.

are 66.0 to 84.5%. In contrast, when the siRNA is delivered with Lipofectamine or Lipofectamine2000, the RAW264.7

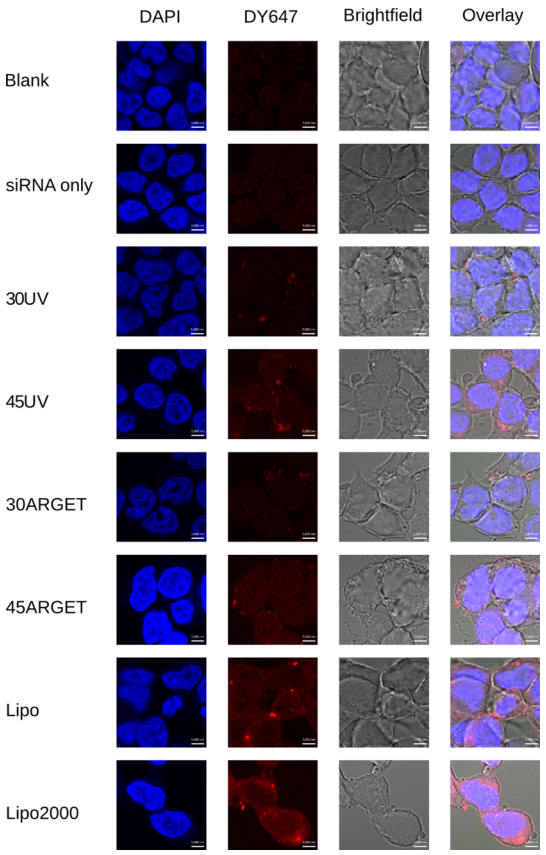

Figure 6. Internalization of fluorescently labeled siRNA in HEK293T cells. Cells were incubated 2 h with 200 nM DY647 fluorescently labeled siRNA complexed with 0.05 mg/mL polycationic nanoparticles or controls prior to rinsing, fixing, DAPI staining, and mounting. Staining of the cells: blue is DAPI stained nuclei, and red is DY647 fluorescently labeled siRNA; 5000 nm scale bars, 63× magnification, $\gamma_{blue} = \gamma_{red} = 0.45$; $\gamma_{bright\text{-}field} = 1.3$.

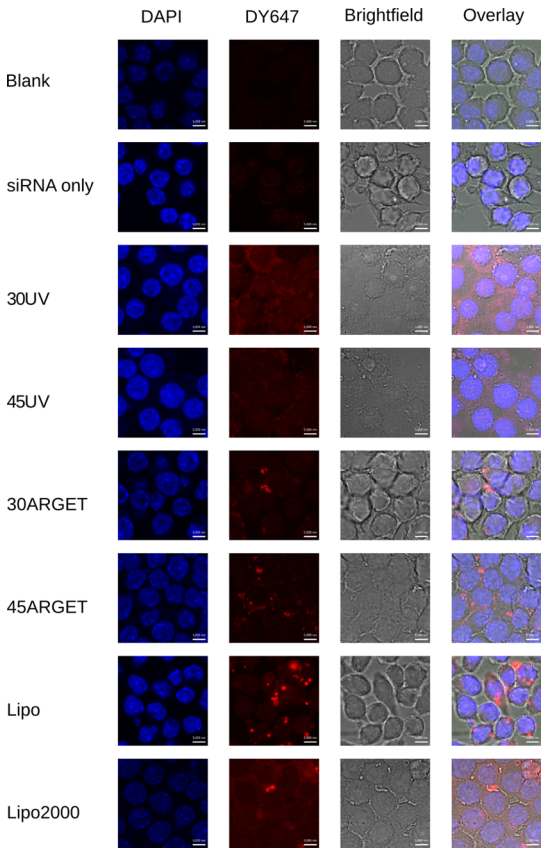

Figure 7. Internalization of fluorescently labeled siRNA in RAW264.7 cells. Cells were incubated 2 h with 200 nM DY647 fluorescently labeled siRNA complexed with 0.05 mg/mL polycationic nanoparticles or controls prior to rinsing, fixing, DAPI staining, and mounting. Staining of the cells: blue is DAPI stained nuclei, and red is DY647 fluorescently labeled siRNA; 5000 nm scale bars, 63× magnification, $\gamma_{blue} = \gamma_{red} = 0.45$; $\gamma_{bright\text{-}field} = 1.3$.

cells do not show increased association compared to HEK293T. Another important difference between the cell types is the no-carrier siRNA-only control, which demonstrates strong association with the HEK293T cells but not the RAW264.7 cells. The cause of this cell-specific association is unclear, as naked siRNA is negatively charged, and thus generally tends to resist association with or transport through the negatively charged cell membrane. Note that uptake of naked siRNA is not without precedent; early knockdown studies were sufficiently promising to motivate clinical trials using naked siRNA, although later studies have relied upon carrier-mediated delivery.[5] Likewise, uptake of naked siRNA has been observed in the literature by Santel *et al.*[20] (who "surprisingly" observed a "significant uptake of fluorescently labeled siRNAs in the absence of transfection reagents" for human HUVEC and HeLa cell lines) and by Petrova *et al.* (who observed an association of naked fluorescently labeled siRNA with HEK293 cells using flow cytometry but not significant uptake with confocal microscopy).[21] Santel *et al.* also observed that the majority of the fluorescence corresponding to the naked siRNA was detected in late endosomal/lysosomal vehicles rather than escaping the endosomal pathway.[20]

For both cell types, 45UV and 45ARGET demonstrate greater normalized fluorescence intensity than the corresponding 30UV and 30ARGET formulations. The formulation 45ARGET demonstrates the largest normalized fluorescence intensity of the four polycationic nanoparticle formulations. Although the difference is slight between the normalized fluorescent intensity for the polycationic nanoparticle formulations between cell types, as a function of normalized fluorescence intensity, the Lipofectamine and Lipofectamine2000 have a much larger signal for the HEK293T cells than for the RAW264.7. Also, the Lipofectamine and Lipofectamine2000 have greater normalized fluorescent intensities than the polycationic nanoparticle formulations.

Confocal Microscopy To Verify siRNA Internalization. Flow cytometry does not distinguish between surface-bound and internalized fluorescence signal, so confocal microscopy was used to verify siRNA internalization. HEK293T cells or RAW264.7 cells were incubated 2 h with DY647 fluorescently labeled siRNA complexed with polycationic

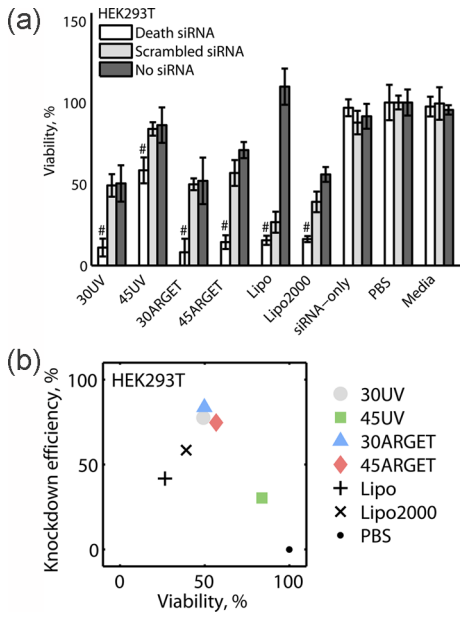

Figure 8. Delivery of AllStars Death siRNA to HEK293T cells using polycationic nanoparticle carriers. The complexes were added to cells at a final concentration of 0.025 mg/mL and 200 nM in the wells following 1 h incubation with Opti-MEM. The polycationic nanoparticles were evaluated *versus* Lipofectamine (0.25 μL/well), Lipofectamine2000 (0.25 μL/well), and no-carrier controls with an MTS assay following 48 h incubation. Pound signs (#) in (a) represent $p < 0.015$ as determined using Student's *t* test.

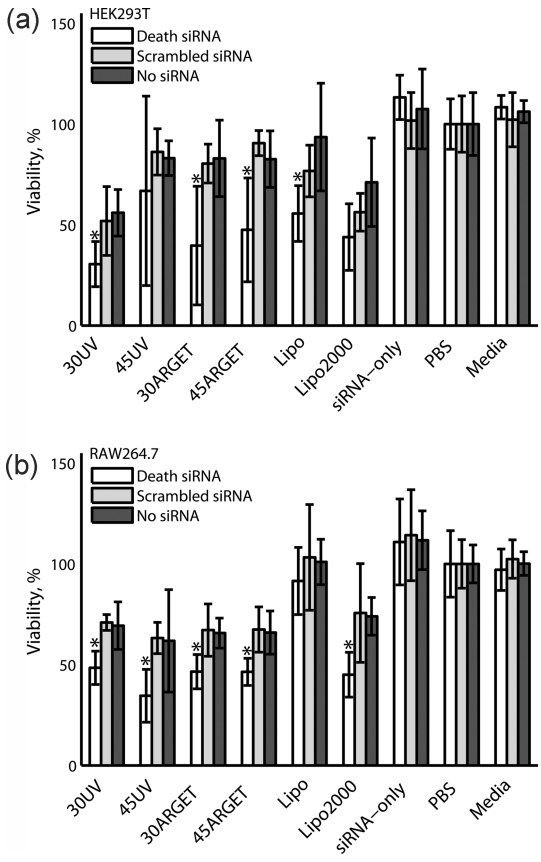

Figure 9. Delivery of AllStars Death siRNA to (a) HEK293T or (b) RAW264.7 cells using polycationic nanoparticle carriers. The complexes were added to cells at a final concentration of 0.025 mg/mL and 100 nM in the wells following 1 h incubation with Opti-MEM. The polycationic nanoparticles were evaluated *versus* Lipofectamine (0.25 μL/well), Lipofectamine2000 (0.25 μL/well), and no-carrier controls with an MTS assay following 48 h incubation. Asterisks (*) represent $p < 0.05$ as determined using Student's *t* test.

nanoparticles or controls (200 nM siRNA and 0.05 mg/mL polycationic nanoparticles). Cells were rinsed, fixed, stained with DAPI nuclear stain, and then mounted to microscope slides. Settings for image acquisition and processing were kept consistent during the experiment for each cell type to permit direct comparisons within each cell type.

The trends observed with flow cytometry are supported by confocal microscopy. Representative images for the HEK293T and RAW264.7 confocal microscopy experiments are shown in Figure 6 and Figure 7, respectively. For the HEK293T cells, visual inspection confirms greater DY647 fluorescence for the 45UV and 45ARGET formulations compared to the corresponding 30UV and 30ARGET formulations. Likewise, the Lipofectamine and Lipofectamine2000 images show more DY647 fluorescence than the polycationic nanoparticles. These microscopy results are consistent with the flow cytometry results. Interestingly, the microscopy results for the 30UV and 45UV suggest a diffuse fluorescence rather than the punctate fluorescence observed for the 30ARGET and 45ARGET formulations. Punctate (speckled or spotted) fluorescence demonstrates a nonhomogeneous distribution of the siRNA in the cytosol, which in turn suggests subcellular localization of the siRNA. Diffuse fluorescence, as for siRNAs that are evenly distributed in the cytosol, suggests endosomal escape.[22] The results of the flow cytometry and confocal microscopy experiments using fluorescently labeled siRNA indicate evidence of internalization necessary for siRNA-induced knockdown.

Transfection with AllStars Death siRNA. Knockdown efficiency induced by siRNA was evaluated using AllStars Hs Cell Death siRNA or AllStars Mm/Tn Cell Death siRNA. HEK293T cells were transfected for 48 h with 0.025 mg/mL polycationic nanoparticles (or appropriate controls) and 100 or 200 nM siRNA following 1 h incubation with Opti-MEM. Cell death was confirmed visually, and viability was evaluated using an MTS assay. The ability of the polycationic nanoparticles to effectively deliver siRNA was first demonstrated in HEK293T cells with 0.025 mg/mL polycationic nanoparticles and 200 nM AllStars Hs Cell Death siRNA (see Figure 8). All of the siRNA delivery carriers demonstrated knockdown, with the greatest efficiency demonstrated by the 30UV, 30ARGET, and 45ARGET formulations (78, 84, and 75% knockdown efficiency, respectively). Unfortunately, this increased knockdown efficiency is associated with decreased cell viability. When the polycationic nanoparticle is kept constant at 0.025 mg/mL and the siRNA concentration is

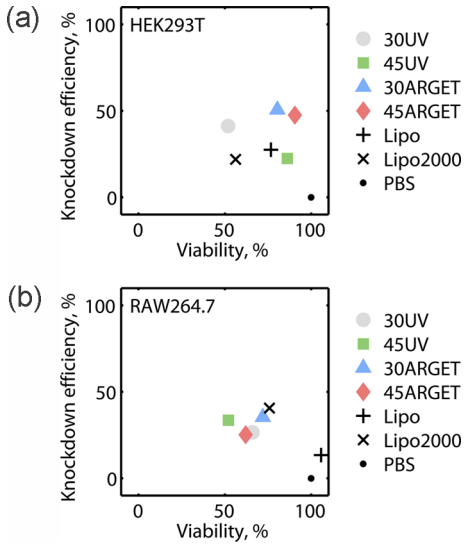

Figure 10. Knockdown efficiency *versus* viability for (a) HEK293T or (b) RAW264.7 cells. Knockdown efficiency was evaluated following 48 h transfection with 0.025 mg/mL polycationic nanoparticles and 100 nM siRNA following 1 h incubation with Opti-MEM. The polycationic nanoparticles were evaluated *versus* Lipofectamine (0.25 μL/well), Lipofectamine2000 (0.25 μL/well), and no-carrier controls.

decreased to 100 nM, the HEK293T cells with scrambled siRNA demonstrate improved viability; as a result, later studies used this 100 nM siRNA concentration (see Figure 9a and Figure 10a). While this change results in increased HEK293T cell viability, it also results in decreased knockdown efficiency and increased variation. There was statistically significant knockdown ($p < 0.05$) for the 30UV, 30ARGET, and 45ARGET formulations (41, 51, and 48%, respectively) as well as the Lipofectamine commercially available transfection agent (28% knockdown).

Knockdown in RAW264.7 cells using 100 nM AllStars Mm/Tn Cell Death siRNA was evaluated using the four nanoparticle formulations as well as two commercially available transfection agents Lipofectamine and Lipofectamine2000 (see Figure 9b and Figure 10b). Statistically significant knockdown ($p < 0.05$) was observed for all four nanoparticle formulations (knockdown efficiency of 27, 34, 35, and 25%, respectively) and also for the Lipofectamine2000 control (41%). The RAW264.7 cells are considered to be more difficult to transfect than HEK293T cells, and this is supported by the decreased transfection efficiency and cell viability with the RAW264.7 cells compared to the HEK293T. Note that dramatically increased transfection efficiency has been observed in 3D cell culture models compared to 2D models,[23] so the next step in evaluating the polycationic nanoparticles and determining a relevant therapeutic concentration of siRNA/polycationic nanoparticles would require improved transfection models such as 3D cell culture or *in vivo* experiments.

CONCLUSIONS

The purpose of the studies undertaken in this report was to provide an analysis of four formulations of polycationic nanoparticles and examine their suitability as siRNA delivery vehicles to HEK293T and RAW264.7 cells. The polycationic nanoparticles demonstrate effective siRNA loading and good biocompatibility at low concentrations *in vitro*. Uptake experiments using flow cytometry and confocal microscopy confirmed siRNA internalization using fluorescently labeled siRNA loaded in polycationic nanoparticles. The percent of cells with fluorescently labeled siRNA uptake was similar across the four formulations, with the RAW264.7 cells demonstrating a greater percent of cells with fluorescently labeled siRNA than the HEK293T cells. However, although all four formulations led to approximately the same percent of cells with fluorescently labeled siRNA, the 45ARGET formulation demonstrated a greater normalized fluorescence intensity than the other polycationic nanoparticle formulations. Knockdown experiments demonstrated knockdown following transfection, with the nanoparticle formulations performing on par with the commercially available carriers. This work indicates that the polycationic nanoparticles may have utility as siRNA delivery vehicles, but additional research is needed to improve knockdown at lower concentrations of siRNA.

METHODS

Chemicals. Poly(ethylene glycol) methyl ether methacrylate (PEGMA) solution (M_n 2000 for PEG chain, 50 wt % in water), 2-(diethylamino)ethyl methacrylate (DEAEMA), *tert*-butyl methacrylate (tBMA), tetraethylene glycol dimethacrylate (TEGDMA), ethyl 2-bromoisobutyrate (EBIB), tris(2-pyridylmethyl)amine (TPMA), ascorbic acid (AA), trypsin-EDTA solution, and Dulbecco's phosphate buffered saline (DPBS, Sigma-Aldrich) were purchased from Sigma-Aldrich. Hydrochloric acid (1 N HCl) was purchased from Fisher Scientific. Copper(II) bromide was purchased from Acros Organics. Ultrapure water was used for all studies. All chemicals were used as received.

Nanoparticle Synthesis and Purification. P(DEAEMA-*co*-tBMA-*co*-PEGMA-*co*-TEGDMA) polycationic nanoparticles were synthesized using a previously reported activators regenerated by electron transfer atom transfer radical polymerization (ARGET ATRP) technique[16,17] or a UV-initiated polymerization technique previously developed by Fisher and colleagues.[18] Briefly, reagents DEAEMA/PEGMA/TEGDMA/$CuBr_2$/TPMA/EBIB at molar ratios of 100:10:4:0.5:0.5:4 (with tBMA with a molar ratio of 30 or 45 depending on the formulation) were combined with 8 mg/mL Brij 30 (Acros Organics) and 1.35 mg/mL myristyltrimethylammonium bromide (MyTab, Sigma-Aldrich) in water for a 0.1 weight ratio of monomer to solvent. For the UV-initiated polymerization, Irgacure 2959 (Ciba) was added at a 0.005 mass ratio of initiator to monomer in place of $CuBr_2$/TPMA/EBIB.

Following probe sonication (S-4000 Misonix Ultrasonicator, Misonix Inc.) and nitrogen purge, the ARGET ATRP and UV-initiated

polymerizations were reacted at ambient temperature for 3 h by the addition of degassed ascorbic acid solution as a reducing agent (AA/DEAEMA 0.5:100) or for 2.5 h by exposure to UV light (Dymax BlueWave200 UV), respectively. Purification was done by a technique described previously by Fisher and Peppas[19] as well as Liechty and colleagues[24] with repeated precipitation/resuspension with acetone/0.5 N HCl. Following dialysis (12000−14000 molecular weight cutoff regenerated cellulose tubing, Spectra/Por), polymer was recovered by freeze-drying.

Binding of siRNA. Nanoparticles were loaded with AllStars negative control siRNA (Qiagen) in 1× PBS pH 5.5 (0.125 mg/mL nanoparticles and 500 nM siRNA). Nuclease free 10× PBS was prepared by dissolving sodium chloride, potassium chloride, monosodium phosphate monohydrate, and disodium phosphate heptahydrate (Fisher Scientific) in water, treating with 0.1% v/v diethylpyrocarbonate (DEPC, Fisher Scientific) overnight, and then autoclaving to remove DEPC. The bound siRNA was determined within 10 min of combining the siRNA with the nanoparticles and then again after 70 and 160 min in order to evaluate the effect of loading time. The siRNA binding was also evaluated at 0.025 mg/mL nanoparticles and 100 nM siRNA in 0.2× PBS pH 5.5, 1× PBS pH 5.5, 1× PBS pH 7.4, and Opti-MEM (reduced serum medium, no Phenol Red, Life Technologies) at approximately 30 min after combining the siRNA with the nanoparticles in order to evaluate the amount of siRNA released in conditions prior to uptake by cells.

The fraction of bound siRNA was determined using a Quant-iT RiboGreen RNA assay kit (Life Technologies) that was adapted for 384-well low-volume plates. Briefly, a 10 μL sample was combined with 10 μL of RiboGreen assay solution (RiboGreen reagent diluted 200× in 1× TE buffer) in a black 384-well low-volume plate. The fluorescence intensity (F) was measured using a microplate reader (Synergy HT, BioTek Instruments, Inc.) 2−5 min after adding the RiboGreen assay solution with 485 nm excitation and 528 nm emission. The RiboGreen reagent is sensitive to components other than RNA present in the assay (although the importance of these contributions diminished for increasing siRNA concentrations), so these contributions to the fluorescence were subtracted from the measured fluorescence signal to calculate the percent of loading (L) in eq 1:

$$L = 100 \times \left(1 - \frac{F_{\text{nanoparticle + siRNA complex}} - F_{\text{nanoparticle only}}}{F_{\text{siRNA only}} - F_{\text{buffer only}}}\right) \quad (1)$$

Cell Culture. Human embryonic kidney 293T cells (HEK293T) and murine macrophage RAW264.7 cells (obtained from American Type Culture Collection) were maintained in Dulbecco's modified Eagle's medium high glucose without L-glutamine (Sigma-Aldrich) supplemented with 1% L-glutamine (MediaTech), 1% penicillin (Sigma-Aldrich), 1% streptomycin (Sigma-Aldrich), and 10% HyClone USDA tested fetal bovine serum (FBS, Thermo Scientific). Opti-MEM reduced serum medium, no Phenol Red (Life Technologies), was used for all cytotoxicity and transfection experiments. Lipofectamine and Lipofectamine2000 (Life Technologies) were used as controls in transfection experiments.

Nanoparticle Cytotoxicity. HEK293T cells were seeded at 5000 cells/well on fibronectin-coated (Sigma-Aldrich) 96-well plates (0.4 μg/well in 75 μL/well DPBS for 45 min), and RAW264.7 cells were seeded at 10000 cells per well in 96-well plates without fibronectin coating (Nunc, Thermo Scientific). After 18 h incubation, the medium was replaced with Opti-MEM. The nanoparticles were prepared at 5× concentration in 1× PBS pH 5.5 and then added to cells at a final concentration of 1× in the wells following 1 h incubation with Opti-MEM.

Following 48 h incubation, medium was removed and cells were incubated for 90 min with CellTiter 96 AQueous nonradioactive cell proliferation assay (MTS, Promega) with serum-free DMEM without Phenol Red (Sigma-Aldrich). The absorbance (A) at 690 nm (background) and 490 nm (MTS assay) was measured using a microplate reader (Synergy HT, BioTek Instruments, Inc.), and cell relative viability (V) was calculated as shown in eq 2:

$$V = \frac{A_{490,\text{sample}} - A_{690,\text{sample}} - (A_{490,\text{nocells}} - A_{690,\text{nocells}})}{(A_{490,\text{media}} - A_{690,\text{media}} - A_{490,\text{nocells}} - A_{690,\text{nocells}})} \quad (2)$$

Flow Cytometry To Quantify Uptake of Fluorescently Labeled siRNA. Flow cytometry was used to quantify siRNA internalization. Flow cytometry measurements were collected using a BD Fortessa flow cytometer and analyzed using FACSDiva software (BD Biosciences). Either 120000 HEK293T cells or 240000 RAW264.7 cells were plated in 6-well plates (Nunc, Thermo Scientific) and incubated for 40 h. Next, cells were incubated for 2 h with 0.05 mg/mL polycationic nanoparticles or appropriate controls with 200 nM fluorescently labeled DY647 siRNA (Thermo Scientific). Controls included Lipofectamine and Lipofectamine2000 (5 μL/well) as well as siRNA-only and untreated controls. Following incubation, cells were rinsed twice with cold 1× DPBS pH 7.4 prior to treating with trypsin (HEK293T) or scraping (RAW264.7) to form a cell suspension. The cell suspension was centrifuged, the supernatant discarded, pellet resuspended in flow cytometry buffer (1% FBS in DPBS), centrifuged again, supernatant discarded, and finally the pellet resuspended in flow cytometry buffer. The samples were stored in darkness at 4 °C before measurement. The results are reported in two ways: as the average percent of cells (taken over a large number of cells, typically 10000) containing fluorescently labeled DY647 siRNA and as the mean fluorescence intensity of the sample normalized to the fluorescence intensity of the blank control. All results are reported as the average plus or minus the standard deviation of three independent experiments. The results for the normalized fluorescence for each cell type were compared by Student's t test (two-tailed, unequal variance) to check for statistically significant differences in the uptake of fluorescently labeled siRNA compared to the no-carrier siRNA-only control.

Confocal Microscopy To Verify siRNA Internalization. Coverslips (18 mm round, no. 1.5 thickness) were acid-washed overnight with 1 N HCl at 60 °C, rinsed with ethanol/water mixtures with successively increasing volume ratios of ethanol, and then the coverslips were placed in a 12-well plate. Prior to plating the HEK293T cells, the acid-washed coverslips in a 12-well plate were coated with fibronectin (4 μg fibronectin/well in 750 μL/well DPBS); no fibronectin coating was used for the RAW264.7 cells. HEK293T and RAW264.7 cells were added at 40000 and 80000 cells/well, respectively. Cells were incubated for 40 h prior to 2 h incubation with 0.05 mg/mL polycationic nanoparticles or appropriate controls with 200 nM siRNA. Controls included Lipofectamine and Lipofectamine2000 (2.5 μL/well) as well as siRNA-only and untreated controls. Following incubation, cells were rinsed three times with 1× PBS pH 7.4 and fixed with 4% paraformaldehyde in 1× DPBS for 10 min prior to washing three times with HBSS (BioWhittaker) and once with DI water (autoclaved). Coverslips were mounted to glass slides using Prolong Gold antifade reagent with DAPI (Life Technologies) and stored in the freezer prior to imaging.

Confocal images were acquired using a Zeiss LSM 710 confocal microscope with a 63× objective. The gain and offset for the different channels were kept constant for the full series of images of each cell type (with the settings for the HEK293T and RAW264.7 cell types optimized separately) to permit image comparisons. Images were collected in 16 bit format, and all images underwent identical postprocessing (γ = 0.45 for red and blue channels, γ = 0.1.3 for bright-field, and bright-field scale adjusted to max/min using ZEN Blue).

Transfection with AllStars Death siRNA. Transfection conditions were matched to those used for cytotoxicity. HEK293T cells were seeded at 5000 cells/well on fibronectin-coated (Sigma-Aldrich) 96-well plates (0.4 μg/well fibronectin in 75 μL/well DPBS for 45 min), and RAW264.7 cells were seeded at 10000 cells per well in 96-well plates without fibronectin coating (Nunc, Thermo Scientific). After 18 h incubation, the medium was replaced with Opti-MEM. The nanoparticles were combined with siRNA (AllStars Hs Cell Death siRNA or AllStars Mm/Tn Cell Death siRNA, Qiagen) in 1× PBS pH 5.5 at 0.125 mg/mL nanoparticles and 5× the final siRNA concentration. The complexes were added to cells at a final concentration of 0.025 mg/mL in the wells (with 100 or 200 nM siRNA) following 1 h incubation with Opti-MEM. Lipofectamine and Lipofectamine2000 wells contained 0.25 μL/well Lipofectamine or Lipofectamine2000. Following 48 h incubation, medium was removed and cell death visually confirmed. Viability was evaluated as for cytotoxicity experiments (cells were incubated for

90 min with MTS solution, and the absorbance was measured with a plate reader). The results for viability for the AllStars Death and the scrambled siRNA were compared by Student's *t* test (two-tailed, unequal variance) to check for statistically significant knockdown. The knockdown efficiency was evaluated using the cell viability (*V*) ratio of cells with death siRNA and cells with scrambled siRNA as shown in eq 3:

$$\% \text{ knockdown} = 100 \times \left(1 - \frac{V_{\text{death}}}{V_{\text{scrambled}}}\right) \quad (3)$$

Conflict of Interest: The authors declare no competing financial interest.

Acknowledgment. This research was supported in part by grants from the National Science Foundation (CBET-1033746) and the Fletcher Stuckey Pratt Chair in Engineering. D.C.F. acknowledges support from the National Science Foundation Graduate Research Fellowship Program (DGE-1110007). The authors thank the Microscopy and Imaging Facility of the Institute for Cellular and Molecular Biology at The University of Texas at Austin for the use of their facilities. Technical support by Biomedical Engineering Undergraduate Researcher H. Frizzell is acknowledged. Helpful discussions with Drs. C. Ellison and D. Paul of The University of Texas at Austin are thankfully acknowledged.

Supporting Information Available: Representative flow cytometry plots are given in the Supporting Information. This material is available free of charge *via* the Internet at http://pubs.acs.org.

REFERENCES AND NOTES

1. Bouchie, A. Companies in Footrace To Deliver RNAi. *Nat. Biotechnol.* **2012**, *30*, 1154–1157.
2. Kang, H. C.; Huh, K. M.; Bae, Y. H. Polymeric Nucleic Acid Carriers: Current Issues and Novel Design Approaches. *J. Controlled Release* **2012**, *164*, 256–264.
3. Kriegel, C.; Attarwala, H.; Amiji, M. Multi-compartmental Oral Delivery Systems for Nucleic Acid Therapy in the Gastrointestinal Tract. *Adv. Drug Delivery Rev.* **2013**, *65*, 891–901.
4. Rehman, Z.; Zuhorn, I. S.; Hoekstra, D. How Cationic Lipids Transfer Nucleic Acids into Cells and across Cellular Membranes: Recent Advances. *J. Controlled Release* **2013**, *166*, 46–56.
5. Forbes, D. C.; Peppas, N. A. Oral Delivery of Small RNA and DNA. *J. Controlled Release* **2012**, *162*, 438–445.
6. Cejka, D.; Losert, D.; Wacheck, V. Short Interfering RNA (siRNA): Tool or Therapeutic?. *Clin. Sci.* **2006**, *110*, 47.
7. Singh, S.; Narang, A. S.; Mahato, R. I. Subcellular Fate and Off-Target Effects of siRNA, shRNA, and miRNA. *Pharm. Res.* **2011**, *28*, 2996–3015.
8. Lindow, M.; Vornlocher, H.; Riley, D.; Kornbrust, D. J.; Burchard, J.; Whiteley, L. O.; Kamens, J.; Thompson, J. D.; Nochur, S.; Younis, H.; *et al.* Assessing Unintended Hybridization-Induced Biological Effects of Oligonucleotides. *Nat. Biotechnol.* **2012**, *30*, 920–923.
9. Soutschek, J.; Akinc, A.; Bramlage, B.; Charisse, K.; Constien, R.; Donoghue, M.; Elbashir, S.; Geick, A.; Hadwiger, P.; Harborth, J.; *et al.* Therapeutic Silencing of an Endogenous Gene by Systemic Administration of Modified siRNAs. *Nature* **2004**, *432*, 173–178.
10. Bartlett, D. W.; Davis, M. E. Effect of siRNA Nuclease Stability on the *In Vitro* and *In Vivo* Kinetics of siRNA-Mediated Gene Silencing. *Biotechnol. Bioeng.* **2007**, *97*, 909–921.
11. Dykxhoorn, D. M.; Palliser, D.; Lieberman, J. The Silent Treatment: siRNAs as Small Molecule Drugs. *Gene Ther.* **2006**, *13*, 541–552.
12. Whitehead, K. A.; Langer, R.; Anderson, D. G. Knocking Down Barriers: Advances in siRNA Delivery. *Nat. Rev. Drug Discovery* **2009**, *8*, 129–138.
13. Marine, S.; Freeman, J.; Riccio, A.; Axenborg, M.; Pihl, J.; Ketteler, R.; Aspengren, S. High-Throughput Transfection of Differentiated Primary Neurons from Rat Forebrain. *J. Biomol. Screening* **2012**, *17*, 692–696.
14. Bertram, B.; Wiese, S.; von Holst, A. High-Efficiency Transfection and Survival Rates of Embryonic and Adult Mouse Neural Stem Cells Achieved by Electroporation. *J. Neurosci. Methods* **2012**, *209*, 420–427.
15. Carralot, J.; Kim, T.; Lenseigne, B.; Boese, A. S.; Sommer, P.; Genovesio, A.; Brodin, P. Automated High-Throughput siRNA Transfection in Raw 264.7 Macrophages: A Case Study for Optimization Procedure. *J. Biomol. Screening* **2009**, *14*, 151–160.
16. Forbes, D. C.; Creixell, M.; Frizzell, H.; Peppas, N. A. Polycationic Nanoparticles Synthesized Using ARGET ATRP for Drug Delivery. *Eur. J. Pharm. Biopharm.* **2013**, *84*, 472–478.
17. Forbes, D. C.; Peppas, N. A. Differences in Molecular Structure in Cross-Linked Polycationic Nanoparticles Synthesized Using ARGET ATRP or UV-Initiated Polymerization. *Polymer* **2013**, *54*, 4486–4492.
18. Fisher, O. Z.; Kim, T.; Dietz, S. R.; Peppas, N. A. Enhanced Core Hydrophobicity, Functionalization and Cell Penetration of Polybasic Nanomatrices. *Pharm. Res.* **2008**, *26*, 51–60.
19. Fisher, O. Z.; Peppas, N. A. Polybasic Nanomatrices Prepared by UV-Initiated Photopolymerization. *Macromolecules* **2009**, *42*, 3391–3398.
20. Santel, A.; Aleku, M.; Keil, O.; Endruschat, J.; Esche, V.; Fisch, G.; Dames, S.; Löffler, K.; Fechtner, M.; Arnold, W.; *et al.* A Novel siRNA-Lipoplex Technology for RNA Interference in the Mouse Vascular Endothelium. *Gene Ther.* **2006**, *13*, 1222–1234.
21. Petrova, N. S.; Chernikov, I. V.; Meschaninova, M. I.; Dovydenko, I. S.; Venyaminova, A. G.; Zenkova, M. A.; Vlassov, V. V.; Chernolovskaya, E. L. Carrier-Free Cellular Uptake and the Gene-Silencing Activity of the Lipophilic siRNAs Is Strongly Affected by the Length of the Linker between siRNA and Lipophilic Group. *Nucleic Acids Res.* **2012**, *40*, 2330–2344.
22. Qi, L.; Gao, X. Quantum Dot-Amphipol Nanocomplex for Intracellular Delivery and Real-Time Imaging of siRNA. *ACS Nano* **2008**, *2*, 1403–1410.
23. Zoldan, J.; Lytton-Jean, A. K. R.; Karagiannis, E. D.; Deiorio-Haggar, K.; Bellan, L. M.; Langer, R.; Anderson, D. G. Directing Human Embryonic Stem Cell Differentiation by Non-viral Delivery of siRNA in 3D Culture. *Biomaterials* **2011**, *32*, 7793–7800.
24. Liechty, W. B.; Scheuerle, R. L.; Peppas, N. A. Tunable, Responsive Nanogels Containing *t*-Butyl Methacrylate and 2-(*t*-Butylamino)ethyl Methacrylate. *Polymer* **2013**, *54*, 3784–3795.
25. Ghosn, B.; Kasturi, S. P.; Roy, K. Enhancing Polysaccharide-Mediated Delivery of Nucleic Acids through Functionalization with Secondary and Tertiary Amines. *Curr. Top. Med. Chem.* **2008**, *8*, 331–340.
26. Singh, A.; Nie, H.; Ghosn, B.; Qin, H.; Kwak, L. W.; Roy, K. Efficient Modulation of T-Cell Response by Dual-Mode, Single-Carrier Delivery of Cytokine-Targeted siRNA and DNA Vaccine to Antigen-Presenting Cells. *Mol. Ther.* **2008**, *16*, 2011–2021.
27. Sun, T.-M.; Du, J.-Z.; Yan, L.-F.; Mao, H.-Q.; Wang, J. Self-Assembled Biodegradable Micellar Nanoparticles of Amphiphilic and Cationic Block Copolymer for siRNA Delivery. *Biomaterials* **2008**, *29*, 4348–4355.
28. Charlaftis, N.; Fearon, D. T.; Schoenemeyer, A.; Morley, P. J. siRNA High-Throughput Kinase Library Screen Identifies Protein Kinase, DNA-Activated Catalytic Polypeptide To Play a Role in MyD88-Induced IFNA2 Activation and IL-8 Secretion. *Biotechnol. Appl. Biochem.* **2012**, *59*, 6–14.
29. Chen, M.; Cooper, H. M.; Zhou, J. Z.; Bartlett, P. F.; Xu, Z. P. Reduction in the Size of Layered Double Hydroxide Nanoparticles Enhances the Efficiency of siRNA Delivery. *J. Colloid Interface Sci.* **2013**, *390*, 275–281.
30. Kim, S.; Ye, C.; Kumar, P.; Chiu, I.; Subramanya, S.; Wu, H.; Shankar, P.; Manjunath, N. Targeted Delivery of siRNA to Macrophages for Anti-inflammatory Treatment. *Mol. Ther.* **2010**, *18*, 993–1001.
31. Wilson, D. S.; Dalmasso, G.; Wang, L.; Sitaraman, S. V.; Merlin, D.; Murthy, N. Orally Delivered Thioketal Nanoparticles Loaded with TNF-α siRNA Target Inflammation

and Inhibit Gene Expression in the Intestines. *Nat. Mater.* **2010**, *9*, 923–928.
32. Laroui, H.; Theiss, A. L.; Yan, Y.; Dalmasso, G.; Nguyen, H. T. T.; Sitaraman, S. V.; Merlin, D. Functional TNFα Gene Silencing Mediated by Polyethyleneimine/TNFα siRNA Nanocomplexes in Inflamed Colon. *Biomaterials* **2011**, *32*, 1218–1228.
33. He, C.; Yin, L.; Tang, C.; Yin, C. Multifunctional Polymeric Nanoparticles for Oral Delivery of TNF-alpha siRNA to Macrophages. *Biomaterials* **2013**, *34*, 2843–2854.
34. McCarthy, J.; O'Neill, M.; Bourre, L.; Walsh, D.; Quinlan, A.; Hurley, G.; Ogier, J.; Shanahan, F.; Melgar, S.; Darcy, R.; *et al.* Gene Silencing of TNF-alpha in a Murine Model of Acute Colitis Using a Modified Cyclodextrin Delivery System. *J. Controlled Release* **2013**, *168*, 28–34.
35. Shrestha, R.; Elsabahy, M.; Florez-Malaver, S.; Samarajeewa, S.; Wooley, K. L. Endosomal Escape and siRNA Delivery with Cationic Shell Crosslinked Knedel-like Nanoparticles with Tunable Buffering Capacities. *Biomaterials* **2012**, *33*, 8557–8568.